

Comparison of Bismuth Stereochemistry in $[\text{BiO}_2]_n$ and $[\text{Bi}_2\text{O}_2]_n$ Layers. Refinement of BiSbO_4

Renée Enjalbert,^a Svetlana Sorokina,^a Alicia Castro^b and Jean Galy^{a,†}

^aCentre d'Elaboration de Matériaux et d'Etudes Structurales, CNRS, 29 rue J. Marvig, 31400 Toulouse, France and ^bInstituto de Ciencia de Materiales de Madrid, CSIC, Serrano 113, 28006 Madrid, Spain

Enjalbert, R., Sorokina, S., Castro, A. and Galy, J., 1995. Comparison of Bismuth Stereochemistry in $[\text{BiO}_2]_n$ and $[\text{Bi}_2\text{O}_2]_n$ Layers. Refinement of BiSbO_4 . – Acta Chem. Scand. 49: 813–819 © Acta Chemica Scandinavica 1995.

Orange transparent single crystals of BiSbO_4 slightly doped by vanadium (<1%) have been synthesized. The structure of this phase, previously described by Aurivillius from rough data using crystal chemistry concepts, has been refined. BiSbO_4 crystallizes in the monoclinic system, space group $I2/c$, $a = 5.4518(8)$, $b = 4.8784(4)$, $c = 11.825(1)$ Å, $\beta = 101.11(1)^\circ$; the final reliability index is $R = 0.059$. The structure contains $[\text{SbO}_4]_n$ layers, formed by SbO_6 octahedra sharing corners, which are parallel to the (001) plane and held together by bismuth atoms. Its general framework is isostructural with $\beta\text{-Sb}_2\text{O}_4$. The precision of the data has allowed one to depict in detail the bismuth coordination polyhedron, a trigonal bipyramid BiO_4E with the lone pair E sitting at one corner of the equatorial triangle. $[\text{BiO}_2]_n$ infinite ribbons develop along the [100] direction and stack in the [010] direction. Structural relationships with structures containing $[\text{Bi}_2\text{O}_2]_n$ layers, in which Bi has a square-pyramidal coordination $[\text{BiO}_4\text{E}]$, are also described.

There has been a renewed interest in bismuth oxide chemistry since the discovery of the remarkable superconductive properties of the phases $\text{Bi}_2\text{Sr}_2\text{Ca}_{n-1}\text{Cu}_n\text{O}_y$ ($n = 1, 2, 3$)¹ or $\text{Ba}_{1-x}\text{K}_x\text{BiO}_3$.² Other phases related to those depicted by Aurivillius, $\text{Bi}_2\text{O}_2(\text{Me}_{m-1}\text{R}_m\text{O}_{3m+1})$, built up by quadratic Bi_2O_2 layers alternating with perovskite layers,^{3,4} exhibit original properties: ferroelectric Bi_2WO_6 ,^{5–7} ferroelastic Sb_2WO_6 ,⁸ the anionic conductor $\text{Bi}_4\text{V}_2\text{O}_{11}$ ⁹ and $\text{Bi}_4\text{V}_2\text{O}_{10}$.¹⁰

Bismuth(III) in these structures possesses a lone pair ($6s^2$) which drastically influences both the stereochemistry and their physical properties. These aspects have been particularly emphasized in our research concerning the chemistry and structural chemistry of the lone pair ns^2 M^* metal oxides (where ns^2 is designated by E), and their combination with transition-metal oxides.^{11–13} The heaviest M^* metals Tl^{I} , Pb^{II} and Bi^{III} behave differently, and it would be reasonable to think that the lone-pair influence is modified by relativistic effects.

Aurivillius's phases are characterized by $[\text{Bi}_2\text{O}_2]_n^{2n+}$ layers structurally identical with the ones found in the red PbO structure. We notice remarkable organization which shows the layer sequence $[\text{E}-\text{Bi}-\text{O}_2-\text{Bi}-\text{E}]_n$. A few studies, however, have been reported on the crystal structure of BiMO_4 ($\text{M} = \text{Nb}, \text{Ta}, \text{Sb}, \text{V}$) compounds, except BiVO_4 .^{14–16} This lack of information is probably due to

experimental difficulties in the preparation of single crystals of good quality. BiNbO_4 , BiTaO_4 and BiSbO_4 have been synthesized by Aurivillius and the BiSbO_4 crystal structure determined.¹⁷ The reliability index R of the structural study was rather high, 0.33 with the heavy atoms and 0.31 when the oxygen atoms were considered. It was difficult with the crystals obtained and the techniques available at that time to lower the R -value.

In our investigations devoted to the compounds having cations with a stereochemical active lone pair of electrons, and more particularly to those containing bismuth, precise information on bond lengths and their stereochemistry is of prior interest in order to contribute to the understanding of its structural chemistry. In this paper we took the opportunity of the successful preparation of good crystals of BiSbO_4 to refine its structure and to develop some structural relationships with related phases.

Experimental

Synthesis. During the attempt to grow crystals in the $\text{Bi}_2\text{O}_3\text{-Sb}_2\text{O}_3\text{-V}_2\text{O}_5$ system, at 800°C for 10 h, transparent single crystals of regular form and orange colour were isolated (Fig. 1). The study of their X-ray diffraction diagrams shows a good agreement with the crystal system, the cell parameters and the space group of BiSbO_4 .¹⁷ An X-ray powder pattern of BiSbO_4 , prepared by heating

[†] To whom correspondence should be addressed.



Fig. 1. Scanning electron micrograph of BiSbO₄ crystals.

appropriate quantities of Bi₂O₃ and Sb₂O₃ at 1000°C for 50 h in air in silica tubes, was perfectly indexed using these data. The orange colour of BiSbO₄ single crystals can be explained by very small V⁵⁺ impurities which could occur during crystal growth. The ternary mixture Bi₂O₃-Sb₂O₃-V₂O₅ probably served as a flux for the crystal growth. This small amount of V⁵⁺ does not change the BiSbO₄ cell parameters significantly (Table 1), and can be assimilated as a very light doping. A similar effect, but giving a green colour, was obtained with tungsten trioxide. In both cases the estimated concentration in V or W is less than 1%.

In Fig. 2 the experimental and calculated powder patterns are compared. A careful analysis of the experimental powder pattern allows the detection of the presence of an impurity (peaks indicated by dots); this impurity was identified as being bismuth silicate Bi₄(SiO₄)₃,¹⁸ this is a result of an attack of the silica tube by Bi₂O₃.

Structure analysis. The data collection was performed using an Enraf-Nonius CAD4 diffractometer. The experimental X-ray data are summarized in Table 2. The intensity of *hkl* reflections were corrected for Lorentz-polarization factors. Bi and Sb atoms were introduced in calculations with proposed Aurivillius fractional coordinates; O(1) and O(2) atoms were localized by a subsequent Fourier difference synthesis. The coordinates and isotropic thermal parameters of the four atoms of the asymmetric unit were refined, the atomic scattering factors being corrected for anomalous dispersion.¹⁹ At this stage the reliability index, *R*, was 0.16.

Table 1. Cell parameters for the BiSbO₄ phase.

Material	<i>a</i> /Å	<i>b</i> /Å	<i>c</i> /Å	β/°
V ₂ O ₅ doping crystal	5.4518(8)	4.8784(4)	11.825(1)	101.11(1)
WO ₃ doping crystal	5.4527(7)	4.8784(8)	11.836(3)	101.12(1)
Pure powder	5.462(2)	4.881(1)	11.828(3)	101.11(6)
Aurivillius crystal	5.464	4.887	11.81	101.0

Table 2. Physical and crystallographic data for BiSbO₄.

Formula	BiSbO ₄
Molecular weight/g	394.7
Morphology	Prismatic block
Dimensions/mm	0.10×0.125×0.075
Crystal system	Monoclinic
Space group	<i>I</i> 2/ <i>c</i>
<i>a</i> /Å	5.4518(8)
<i>b</i> /Å	4.8784(4)
<i>c</i> /Å	11.825(1)
β/°	101.11(1)
<i>V</i> /Å ³	308.61(6)
<i>Z</i>	4
ρ _{calc} /g cm ⁻³	8.47
<i>F</i> (000)	664
μ (MoKα)/cm ⁻¹	626
Wavelength (MoKα)/Å	0.71069
Monochromator	Oriented graphite
Take off/°	3.5
Detector width/mm ²	4×4
Scan type	ω/2θ
Scan width/°	1.0+0.35 tanθ
Prescan speed/° min ⁻¹	10
Maximum time/s	60
Reflections for cell refinement	25; 12 ≤ 2θ ≤ 62°
Recorded reflections	1590; 2θ ≤ 70°
<i>hkl</i> range	-8 ≤ <i>h</i> ≤ 8, 0 ≤ <i>k</i> ≤ 7, 0 ≤ <i>l</i> ≤ 19
Intensity control reflections	400/040/0012 every 3600 s
Orientation control reflections	6-40/106 every 250 reflections

The absorption effects were obviously considerable. In the first attempt, empirical absorption corrections²⁰ were applied. The results are given in Table 3. Negative thermal parameters affecting several atoms were related to an incompletely adapted correction. The numerical absorption correction²¹ has been shown to be more adequate than empirical ones, allowing one to refine the Bi and Sb atoms with their anisotropic thermal parameters. Least-squares refinements were performed in the case of the centrosymmetric space group *I*2/*c* (very strong correlations appear in *Ic*). The secondary extinction correction and various tests of ponderation scheme have not given significant improvement. The final values are presented in Table 4, the positional and thermal parameters in Table 5 and the main interatomic distances and angles in Table 6. The calculations and drawings were performed with the SHEL86²² and ORTEP²³ programs using the Alliant vectorial superminicomputer VFX/80. Based on structural results, a good fit between calculated (LAZY-PULVERIX program)²⁴ and experimental powder patterns was obtained (Fig. 2).

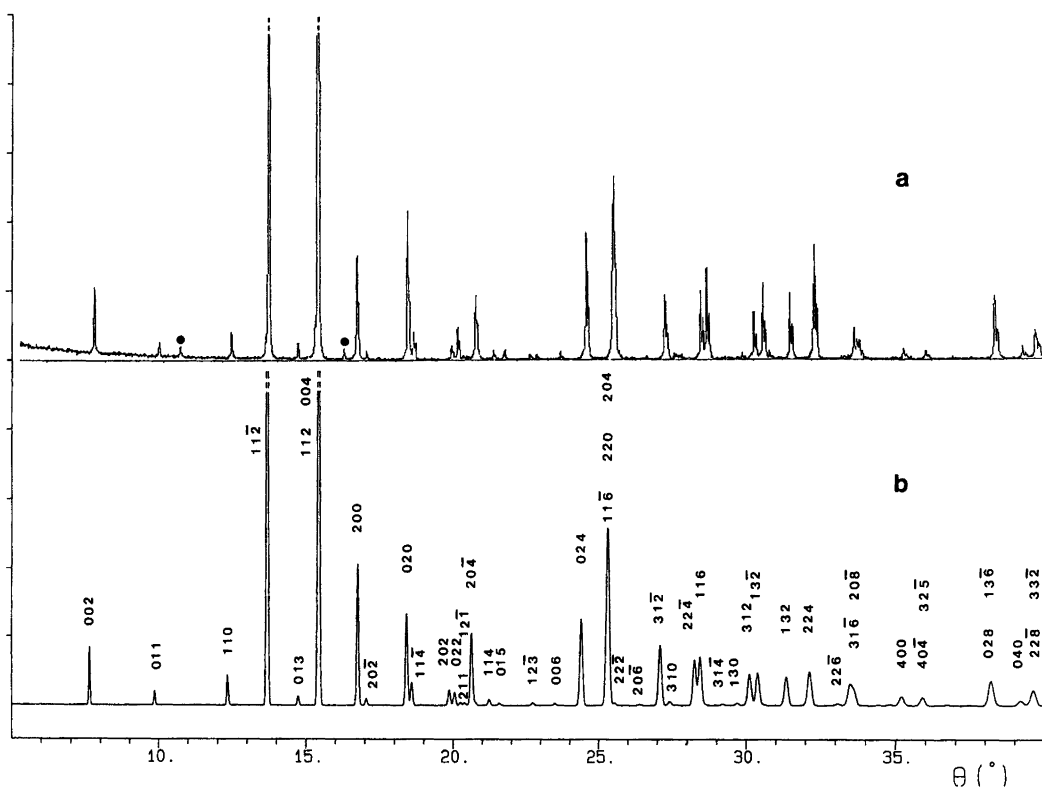


Fig. 2. Experimental (a) and calculated (b) powder patterns of BiSbO₄. The dots indicate the presence of Bi₄(SiO₄)₃.

Discussion

The crystal structure of BiSbO₄ is projected onto the (010) plane in Fig. 3. Examination of Table 6 shows that the values of the Bi–O and Sb–O distances do not differ significantly from those established previously by Aurivillius, in spite of the high *R*-index founded. Such a result shows once again that even if the crystal is of poor quality and absorption correction almost impossible to proceed properly, structural analysis enlightened by a strong crystal-chemistry basis can provide a very reasonable structure.

Six nearest oxygen atoms surround the antimony atoms at distances ranging from 1.98 to 1.99 Å, forming a quasi-regular octahedron (Fig. 4). The antimony oxidation state is clearly +5. Such an observation can be related to the β-Sb₂O₄ features^{25,26} where Sb–O distances

Table 3. Comparison of the empirical and numerical absorption corrections.

Correction mode	Empirical	Numerical
2θ range/°	3–70	3–70
Number of data	498	498
$U_{iso}/\text{Å}^2$		
Bi	0.0065(3)	0.0091(6)
Sb	0.0003(3)	0.0044(7)
O(1)	< 0	0.002(2)
O(2)	0.005(3)	0.008(3)
<i>R</i>	0.063	0.061
<i>R_w</i>	0.074	0.072

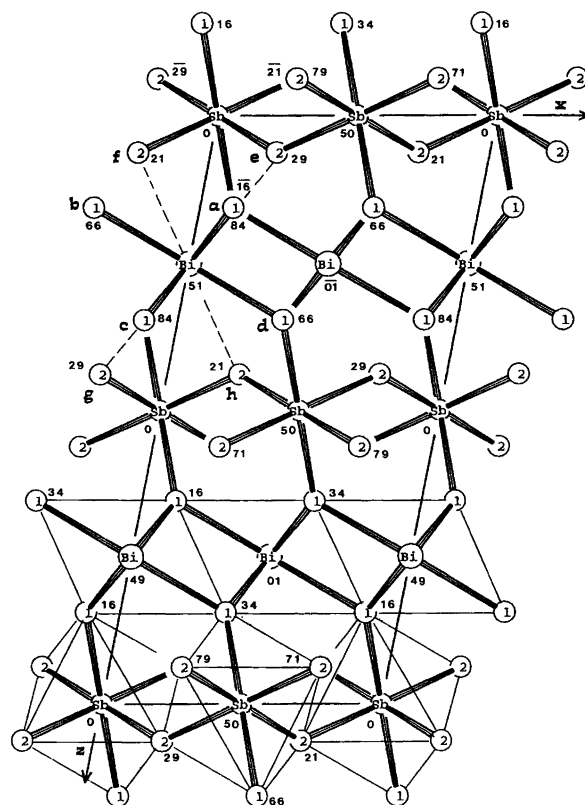


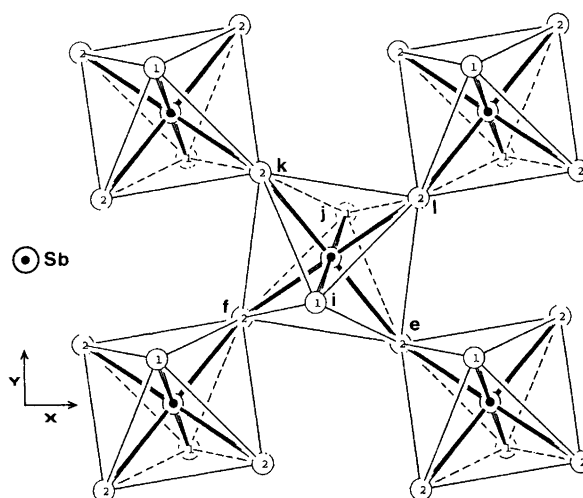
Fig. 3. Projection of the structure of BiSbO₄ onto the (010) plane.

Table 4. Final values after numerical absorption correction.

Absorption coefficient min.–max.	0.016–0.075
Number of unique data with $I > 3\sigma(I)$	453
Number of refined parameters	20
Correlation between parameters	0
Height max. in difference Fourier synthesis at 0.6 Å of Bi atoms	$6 e \text{ \AA}^{-3}$
Reliability factors R	0.059
R_w	0.070

range from 1.97 to 2.0 Å. In a recent investigation of an original compound $\text{Sb}_2\text{Te}_2\text{O}_9$,²⁷ exhibiting $[\text{Sb}_2\text{O}_9]_n$ ribbons built up by regular SbO_6 octahedra, Sb–O distances show a wider range of values, from 1.91 to 2.03 Å.

Bismuth atoms are surrounded by eight oxygen atoms, which are situated at the corners of a square antiprism (Fig. 5a). In the BiO_8 polyhedron, the average Bi–O bond distance is 2.56 Å, with four Bi–O(1) short bonds, 2.13–2.27 Å, and four Bi–O(2) from 2.82 to 2.99 Å. Bismuth atoms may be considered as one-sided, coordinated to four O(1) oxygens situated at the apices of a distorted trigonal bipyramid (TBP), the lone pair occupying one corner of the equatorial triangle. Following the stereo-

Fig. 4. Antimony–oxygen framework, $[\text{SbO}_4]_n$ layers, in BiSbO_4 structure.

chemical analysis previously proposed,¹² the center of the sphere of influence of the lone pair in this BiO_4E bipyramid is at a distance Bi–E = 0.96 Å; the calculated

Table 5. Positional and thermal parameters for BiSbO_4 .

Atom	x	y	z	B_{eq} or $*B_{\text{iso}}/\text{\AA}^2$
Bi	0	0.5125	1/4	0.71(4)
Sb	0	0	0	0.25(6)
*O(1)	0.121(3)	–0.159(3)	0.155(2)	0.2(2)
*O(2)	0.240(3)	0.292(3)	0.062(2)	0.6(2)

Atom	U_{11}	U_{22}	U_{33}	U_{23}	U_{13}	U_{12}	$U_{\text{eq}}/\text{\AA}^2$
Bi	0.0090(5)	0.0080(6)	0.0096(5)	0	0	0.003(3)	0.0089(5)
Sb	0.0033(7)	0.0030(8)	0.0029(7)	0.0005(7)	0.0006(5)	0.0007(7)	0.0031(5)

Table 6. Selected distances (in Å) and angles (in °) for BiSbO_4 .

Bi–O(1)	2.133(7)	$\times 2$ (a,c)
	2.269(8)	$\times 2$ (b,d)
Bi–O(2)	2.818(9)	$\times 2$ (f,h)
	2.989(9)	$\times 2$ (e,g)
O(1)–Bi–O(1)	71.3(7)	$\times 2$ (a–d, b–c)
	81.2(4)	$\times 2$ (a–b, c–d)
	82.6(9)	α (a–c)
	143.3(8)	β (b–d)
O(2)–Bi–O(2)	56.6(4)	$\times 2$ (e–f, g–h)
	99.9(6)	$\times 2$ (e–h, f–g)
	116.4(7)	(f–h)
	137.8(6)	(e–g)
Sb–O(1)	1.983(8)	$\times 2$ (i, j)
Sb–O(2)	1.977(7)	$\times 2$ (e, k)
	1.994(8)	$\times 2$ (f, l)
O(1)–Sb–O(2)	82.0(7)/98.0(7)	$\times 2$ (e–j, k–i)/ $\times 2$ (e–i, j–k)
	87.9(5)/92.1(5)	$\times 2$ (e–f, k–l)/ $\times 2$ (e–l, f–k)
	89.6(8)/90.4(8)	$\times 2$ (i–l, j–f)/ $\times 2$ (i–l, l–j)
O–O	2.57(1)/2.60(1)/2.757(2)	
	2.80(1)/2.82(2)/2.86(2)	
	2.99(1)/3.01(1)	

Symmetry code: (a) $x, 1+y, z$; (b and f) $-1/2+x, 1/2-y, z$; (c) $-x, 1+y, 1/2-z$; (d and h) $1/2-x, 1/2-y, 1/2-z$; (e and j) x, y, z ; (g) $-x, y, 1/2-z$; (i and k) $-x, -y, -z$; (l) $1/2-x, 1/2-y, -z$.

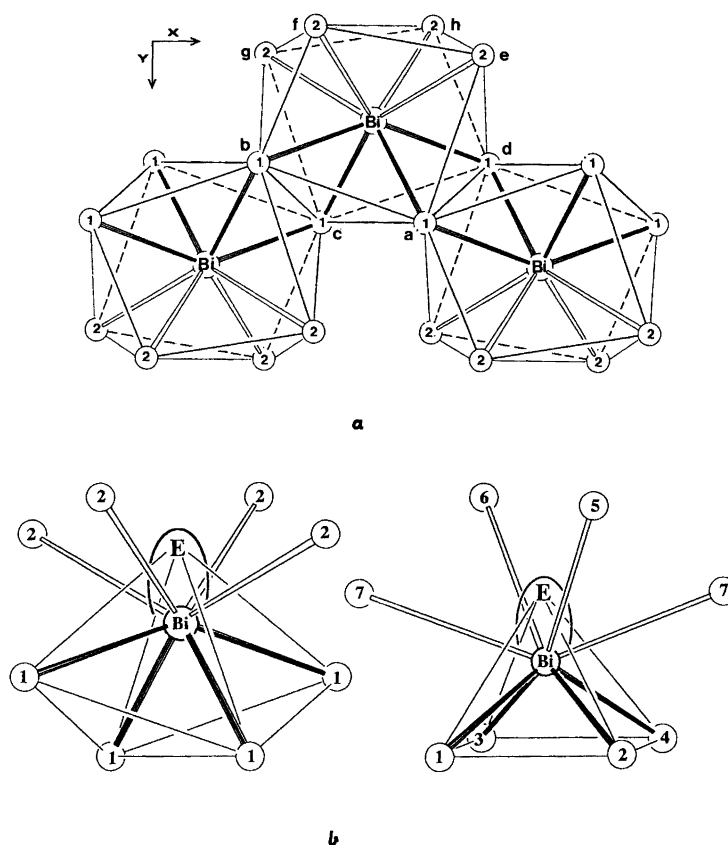


Fig. 5. (a) Infinite $[\text{BiO}_2]_n$ ribbons in BiSbO_4 structure; (b) bismuth in a square antiprism polyhedron, giving a TBP- BiO_4E in BiSbO_4 structure and SP- BiO_4E in $\text{Bi}_4\text{V}_2\text{O}_{10}$ structure.

coordinates of E are 0, 0.32, 1/4; the α - and β -angles are 82.6 and 143.3°, respectively, very close to those observed in $\beta\text{-Sb}_2\text{O}_4$, 87.9 and 148.1°. It is then easy to visualize the Bi environment in the TBP in the BiSbO_4 structure in comparison with the regular square pyramid (SP) found, for example, in the $\text{Bi}_4\text{V}_2\text{O}_{10}$ structure¹⁰ (Fig. 5b). The distribution of Bi-O interatomic distances

can be compared favourably, for example, with those found for Bi^{III} in the compound $\text{Cu}_3\text{Bi}_4\text{V}_2\text{O}_{14}$, whose structure was recently published.²⁸

Coming to the general architecture of BiSbO_4 , which is isostructural with $\beta\text{-Sb}_2\text{O}_4$, it is possible to depict that it is formed by $[\text{SbO}_4]_n$ layers built up by octahedra sharing corners held together via bismuth atoms lying in a (001)

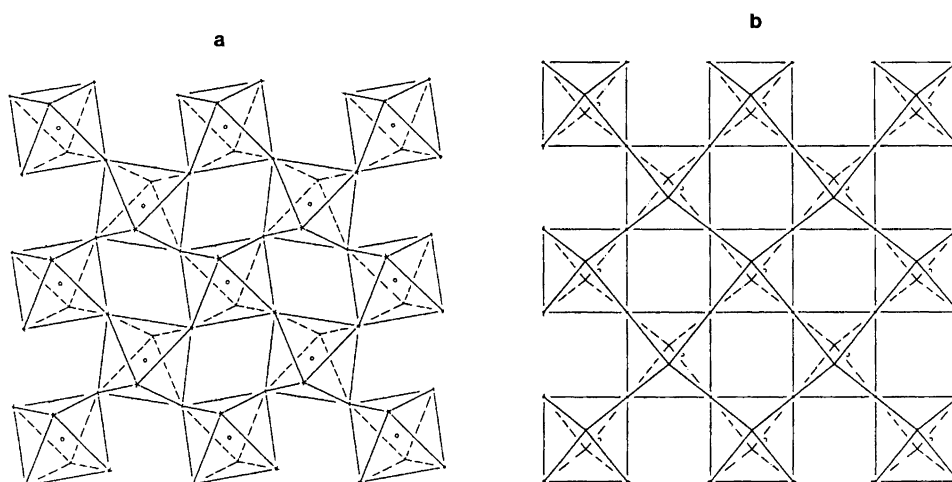


Fig. 6. Comparison between $[\text{SbO}_4]_n$ (a) and $[\text{WO}_4]_n$ (b) layers in BiSbO_4 and Bi_2WO_6 structures.

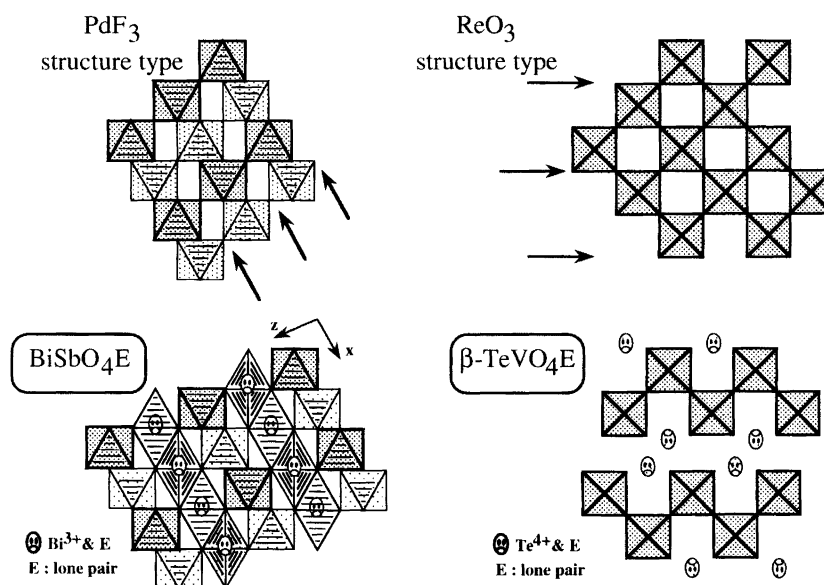


Fig. 7. Two structures BiSbO_4 and $\beta\text{-TeVO}_4$ derived from PdF_3 and ReO_3 structures after the shearing effect of the lone-pair elements Bi^{III} and Te^{IV} .

plane. If the bismuth lone pair E and oxygen atoms are considered together it may be noted that quasi-hexagonal close packing is formed. The $[\text{SbO}_4]_n$ at the opposite of the $[\text{WO}_4]_n$ found in Bi_2WO_6 , for example, is quite different (Fig. 6). It derives from a section of the PdF_3 structure type (hcp), while the $[\text{WO}_4]_n$ layer is similar to SnF_4 layer structure, itself a section of the ReO_3 structure type (the PdF_3 structure type can be considered as the high-pressure form of the ReO_3 structure type).

Formally we wish to consider these lone-pair elements as efficient cutting tools, 'chemical scissors', of various structures.¹¹ In the idealized drawings of Fig. 7 it is shown, as an example, how Bi^{III} or Te^{IV} 'cuts' the (hcp) PdF_3 or ReO_3 structures in order to obtain BiSbO_4 or $\beta\text{-TeVO}_4$ networks.^{29,30}

Looking at the bismuth–oxygen framework and taking into account the strong Bi–O bonds [Bi and O(1) atoms] we note the remarkable infinite ribbons $[\text{BiO}_2]_n$ formed,

which develop along the [100] direction. These ribbons are stacked along the [010] direction weakly bridged by rather long Bi–O bonds ($2.82 < \text{Bi–O} < 2.99 \text{ \AA}$) [Bi and O(2) atoms] (Fig. 8a). If the oxygens below the plane containing Bi atoms are selected, they depict a network (Fig. 8b) which can be rearranged easily in a perfect quadratic oxygen network (Fig. 8c). Only 50% of the squares are capped by Bi atoms forming a $[\text{BiO}_2]_n$ plane. If we imagine an increase of the bismuth and oxygen content in such a BiMO_4 structure, the extra Bi atoms can cut the structure again along planes parallel to (001). They can be fixed on the free side of the previous $[\text{BiO}_2]_n$ layers building the Aurivillius $[\text{Bi}_2\text{O}_2]_n$ layers (Fig. 8d). The oxygen atoms are accommodated by the M element, forming $[\text{MO}_4]_n$ layers. Such layers, instead of staying in the (hcp) form of the $[\text{SbO}_4]_n$ type, can then develop to make the less compact layers of the $[\text{WO}_4]_n$ type as in $(\text{Bi}_2\text{O}_2)\text{WO}_4$, i.e. Bi_2WO_6 .

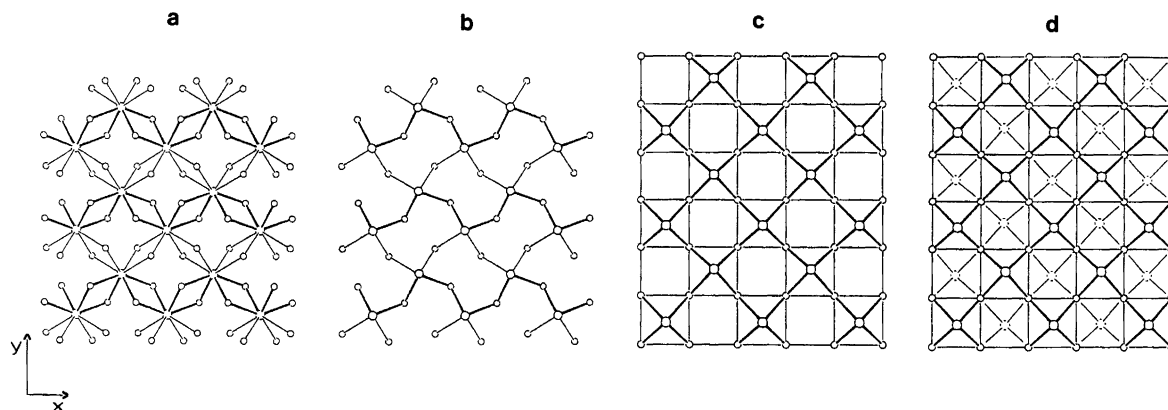


Fig. 8. (a) Bismuth oxygen network in BiSbO_4 ; (b) and (c) part forming $[\text{BiO}_2]_n$ layer and its reorganization; (d) $[\text{Bi}_2\text{O}_2]_n$ layer.

Bengt Aurivillius, in his numerous papers on the structure of compounds or phases containing heavy elements like bismuth, has shown that mastered crystal-chemistry concepts firmly applied in these investigations allow one to derive an exact structure and to depict the stereochemistry of these elements. The refinement of the BiSbO₄ crystal structure performed with advanced techniques on good single crystals provides precise information on the chemical bonding around bismuth atoms as well as on the whole structure, and confirms in every detail the assertions of Aurivillius.

Acknowledgements. We express our gratitude to the CNRS of France and the CSIC of Spain for aid under the International Scientific Cooperation Program (PICS).

References

1. Tarascon, J. M., Le Page, Y., Barboux, P., Bagley, B. G., Greene, L. H., McKinnon, W. R., Hull, G. W., Giroud, M. and Hwang, D. M. *Phys. Rev. B* 37 (1988) 9332.
2. Schneemeyer, L. F., Thomas, S. K., Siegrist, T., Batlogg, B., Rupp, L. W., Opila, R. L., Cava, R. S. and Murphy, D. W. *Nature (London)* 335 (1988) 421.
3. Aurivillius, B. *Arkiv Kemi* 1 (1949) 463.
4. Aurivillius, B. *Arkiv Kemi* 2 (1950) 519.
5. Ismailzade, I. G. and Mirishili, F. A. *Sov. Phys. Crystallogr.* 14 (1970) 636.
6. Newkirk, H. W., Quadflieg, P., Liebertz, J. and Kockel, A. *Ferroelectrics* 4 (1972) 51.
7. Wolfe, R. W., Newnham, R. E. and Kay, M. I. *Solid State Commun.* 7 (1969) 1797.
8. Castro, A., Millan, P., Enjalbert, R., Snoeck, E. and Galy, J. *Mater. Res. Bull.* 29 (1994) 871.
9. Sharma, V., Skukla, A. K. and Gopalakrishnan, J. *Solid State Ionics* 58 (1992) 359.
10. Galy, J., Enjalbert, R., Millan, P. and Castro, A. *C.R. Acad. Sci. Paris* 317 (II) (1993) 43.
11. Galy, J. *NBS Publ.* 364 (1972) 29.
12. Galy, J., Meunier, G., Andersson, S. and Åstrom, A. *J. Solid State Chem.* 13 (1974) 142.
13. Galy, J. and Enjalbert, R. *J. Solid State Chem.* 44 (1982) 1.
14. Keve, E. T. and Skapski, A. C. *J. Solid State Chem.* 8 (1973) 159.
15. Sleight, A. W., Chen, H. Y., Ferretti, A. and Cox, D. E. *Mater. Res. Bull.* 14 (1979) 157.
16. Granzin, J. and Pohl, D. Z. *Kristallogr.* 169 (1984) 289.
17. Aurivillius, B. *Arkiv Kemi* 3 (1951) 153.
18. Bi₄(SiO₄)₃, no. 33-215, *Joint Committee on Powder Diffraction Standards* Swarthmore, PA.
19. Cromer, D. T. and Waber, J. T. *International Tables for X-Ray Crystallography*, Vol IV, Kynoch Press, Birmingham 1974.
20. North, A. C. T., Philips, D. C. and Matthews, F. S. *Acta Crystallogr., Sect. A* 24 (1968) 351.
21. Coppens, P., Leiserowitz, L. and Rabinovich, D. *Acta Crystallogr.* 18 (1965) 1035.
22. Sheldrick, G. M. *Program for Solution of Crystal Structures*, Göttingen, Germany 1986.
23. Johnson, C. K. *Ortep II report ORNL5138*, Oak Ridge Laboratory, TN 1976.
24. Yvon, K., Jeitschko, W. and Parthe, E. *J. Appl. Crystallogr.* 10 (1977) 73.
25. Rogers, D. and Skapski, A. C. *Proc. Chem. Soc.* (1964) 400.
26. Amador, J., Gutierrez Puebla, E., Monge, M. A., Rasines, I. and Ruiz Valero, C. *Inorg. Chem.* 27 (1988) 1367.
27. Alonso, J. A., Castro, A., Enjalbert, R., Galy, J. and Rasines, I. *J. Chem. Soc., Dalton Trans* (1992) 2551.
28. Deacon, G. B., Gatehouse, B. M. and Ward, G. N. *Acta Crystallogr., Sect. C* 50 (1994) 1178.
29. Meunier, G., Darriet, J. and Galy, J. *J. Solid State Chem.* 5 (1972) 314.
30. Meunier, G., Darriet, J. and Galy, J. *J. Solid State Chem.* 6 (1973) 67.

Received December 30, 1994.